



Stretchable lithium-air batteries for wearable electronics†

Lie Wang, Ye Zhang, Jian Pan and Huisheng Peng*

Cite this: *J. Mater. Chem. A*, 2016, 4, 13419Received 11th July 2016
Accepted 9th August 2016

DOI: 10.1039/c6ta05800k

www.rsc.org/MaterialsA

The development of stretchable energy storage devices with a high energy density is critical while it remains a challenge for the next-generation wearable electronics. Lithium-air batteries could theoretically provide a high energy density, but they are generally bulky and inflexible with poor cycle performance as well as exhibit volatilization and leakage of liquid electrolyte, which has largely limited their applications. Herein, for the first time, a new flexible and stretchable lithium-air battery has been developed by designing a rippled air electrode made of aligned carbon nanotube sheets, a lithium array electrode and a polymer gel electrolyte. It exhibits excellent electrochemical properties including high energy density, and the high electrochemical performances are well maintained under various deformations such as bending, twisting and stretching. This lithium-air battery is demonstrated to be promising in a variety of fields, particularly, wearable electronics.

Introduction

Flexible and wearable electronic devices have recently gained increasing popularity, and pointed to promising applications such as artificial skins, epidermal sensors, smart clothes, and implantable medical devices.^{1–6} As a result, the development of suitable energy storage devices to power them is highly required. In contrast to the well-developed rigid format, a highly flexible configuration is desirable to make these devices conform to soft and irregular surfaces of the body to minimize discomfort. Moreover, stable performances of these devices under deformations including bending, twisting and even stretching should be guaranteed.^{7–9} Therefore, they need not only be flexible but also be stretchable. To this end, a lot of effort has been devoted to developing stretchable energy storage devices, *e.g.*, supercapacitors, lithium-ion batteries and alkaline manganese batteries.^{10–14} However, the low theoretical energy

densities of these power devices intrinsically limit their broad applications in wearable devices. Indeed, long lasting batteries seemed to be unattainable for many years,^{15,16} which have therefore significantly impeded the commercialization of wearable devices.

Recently, lithium-air (Li-air) batteries have emerged as a promising candidate due to a high theoretical energy density of about 3500 Wh kg⁻¹, which is 5–10 times higher than conventional lithium-ion batteries.^{17–19} Therefore, the development of stretchable Li-air batteries may meet the requirements of flexibility and high energy density of the wearable devices. However, there remain some critical challenges. Firstly, the Li-air battery is typically packed with bulky and rigid stainless steel.^{20,21} Secondly, the lithium metal electrode and current collector (*e.g.*, carbon paper and nickel foam) are inextensible. Thirdly, it shows a poor cycle performance often with volatilization and leakage of liquid electrolyte during use.^{22,23}

In this communication, for the first time, a new stretchable Li-air battery has been developed with high electrochemical properties by designing a rippled air electrode made of aligned carbon nanotube (CNT) sheets, a lithium array electrode and a polymer gel electrolyte. This Li-air battery exhibited a discharge capacity of 7111 mAh g⁻¹ and could effectively work for 180 cycles in air. Moreover, it is flexible, stretchable and able to sustain thousands of repeated deformations without obvious decay in performance. It was demonstrated as an elastic “energetic strap” to power a sensor suite for wearable physiological monitoring (Fig. 1a).

Experimental section

Fabrication of the stretchable air electrode

An elastic polymer substrate was obtained by injecting a precursor solution of Ecoflex into a template, followed by curing at 80 °C for 2 h. The aligned CNT sheet was directly drawn from a spinnable CNT array and stacked on the pre-stretched polymer substrate, followed by dropping ethanol to enhance the contact between the CNT and polymer substrate.

State Key Laboratory of Molecular Engineering of Polymers, Department of Macromolecular Science and Laboratory of Advanced Materials, Fudan University, Shanghai 200438, China. E-mail: penghs@fudan.edu.cn

† Electronic supplementary information (ESI) available. See DOI: 10.1039/c6ta05800k

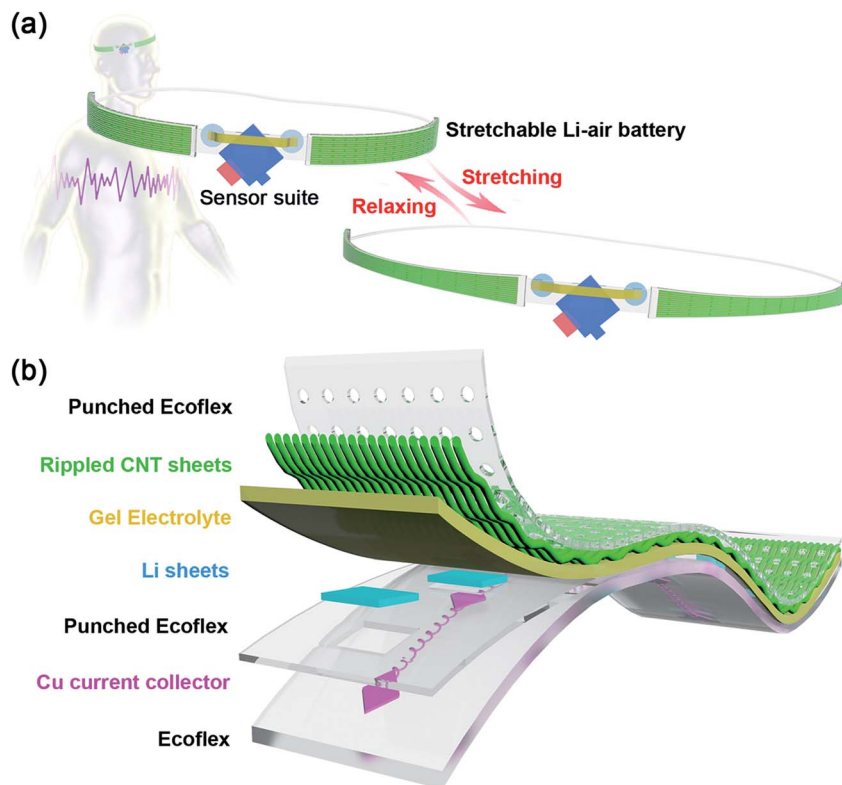


Fig. 1 (a) Potential application of the stretchable Li-air batteries as elastic “energetic straps” to power a sensor suite for wearable physiological monitoring. (b) Multi-layered structure of the stretchable Li-air battery.

Here the CNT exhibits a multi-walled structure with a diameter of about 10 nm.²⁴ The stretchable air electrode was then obtained after releasing the pre-stretched polymer substrate.

Fabrication of the stretchable Li array electrode

A Cu wire (diameter of 50 μm) was wound onto a steel wire with a diameter of 600 μm , followed by removal from the steel wire to form Cu springs. The Cu springs were then connected in series by Cu sheets and paved on a glass substrate, followed by coating an Ecoflex precursor solution. After curing, a stretchable Cu current collector was obtained by peeling off from the glass substrate. The stretchable Cu current collector was then transferred to an argon-filled glovebox. After that, Li sheets were paved on the Cu sheets point-to-point, followed by covering a punched Ecoflex film as a fixed layer to obtain the stretchable Li array electrode.

Preparation of the gel electrolyte

Lithium bis(trifluoromethane)sulfonamide (0.30 g), succinonitrile (0.35 g) and polyethylene oxide (0.35 g) were added to a solution mixture containing methylene chloride (4.0 mL) and acetone (0.10 mL) to form solution A. Poly(vinylidene fluoride-co-hexafluoropropylene) (0.10 g) was dissolved in *N*-methyl-2-pyrrolidinone (0.40 g) to produce solution B. The gel electrolyte was obtained by mixing solutions A and B with strong agitation. All samples were processed and prepared in an argon-filled glovebox.

Fabrication and characterization of the stretchable Li-air battery

A stretchable Li array electrode was coated with a layer of gel electrolyte, followed by attaching with a stretchable air electrode to produce the stretchable Li-air battery. The electrochemical measurements were conducted on an Arbin multichannel electrochemical testing system (MSTAT-5 V/10 mA/16Ch). Electrochemical impedance spectroscopy was carried out on a CHI 660D electrochemical workstation with frequencies ranging from 0.1 Hz to 100 kHz.

Results and discussion

The structure and fabrication of the stretchable Li-air battery are schematically shown in Fig. 1b and S1.† A stretchable air electrode was fabricated by first stacking aligned CNT sheets onto a punched elastic polymer (Ecoflex) film in a pre-stretchable state and then releasing the substrate to its natural state (Fig. S1a†). Here the aligned CNT sheets were directly drawn from a spinnable CNT array synthesized by chemical vapor deposition.²⁴ A stretchable Li array electrode was then fabricated by paving Li sheets on a stretchable Cu current collector, followed by covering a punched Ecoflex film as a fixed layer. The Cu current collector was pre-fabricated by connecting the Cu springs and Cu sheets embedded in an Ecoflex film (Fig. S1b†). The stretchable Li-air battery was finally produced by sandwiching the stretchable air electrode and Li array electrode with a polymer gel electrolyte (Fig. S1c†).

Fig. S2† displays typical scanning electron microscopy (SEM) images of the resulting stretchable air electrode with rippled aligned CNT sheets on the surface. The rippled structure facilitated the stretchability of the air electrode up to a high strain of 100% without decreasing the electrical conductivity (Fig. S3a†). Moreover, the electrical resistance was increased by less than 4% even after 1000 stretching cycles at a strain of 100% (Fig. S3b†), which is derived from the well-maintained rippled structure of the aligned CNT sheets under stretching (Fig. S4†). The embedded Cu spring was used to connect the isolated Li sheets and offered stretchability for the Li array electrode. This Cu spring had been traced before and after stretching (Fig. S5†), and it remained stable without obvious cracks after repeatedly stretching and releasing for 1000 cycles at a strain of 100% (Fig. S5b†).

The electrochemical performances of the Li-air battery were systemically investigated in ambient air with a relative humidity of ~5% at room temperature. Fig. 2a shows that the discharge voltage plateau slightly decreased from 2.68 to 2.64, 2.57 and 2.52 V, with the increasing current densities from 250 to 500, 1000 and 1500 mA g⁻¹, respectively. This indicates that it can be steadily operated at a wide variety of current densities. Moreover, a high capacity of 7111 mAh g⁻¹ was obtained at a current density of 500 mA g⁻¹ (Fig. 2b). Fig. 2c and S6† display the typical voltage profiles cycled at a cutoff capacity of 500 mAh g⁻¹. The specific capacity and discharge voltage plateau remained almost unchanged over 180 cycles (Fig. 2d).

The reaction products of the Li-air battery were also investigated after the discharging and recharging processes. The characteristic peaks of Li₂O₂ at 32.9° and 35° were observed after the first discharge process by X-ray diffraction,²⁵ and they disappeared after the subsequent recharge process (Fig. S7†).

This conclusion was further verified by SEM. Toroidal nanoparticles appeared on the air electrode after the first discharge and then disappeared at the following recharging process (Fig. S8†). These results suggested that the highly reversible Li₂O₂ is the main reaction product in the discharging process. In addition, LiOH and Li₂CO₃ were also detected by X-ray photoelectron spectroscopy with increasing cycles (Fig. S9†). H₂O molecules in air may permeate through the air electrode to react with Li₂O₂ and generate LiOH, and the LiOH then reacted with CO₂ to form Li₂CO₃.²² The accumulation of LiOH and Li₂CO₃ during long-period cycling was associated with the increasing charge overpotential (Fig. 2c) and affected the battery performance,²³ e.g., the electrochemical performance degraded remarkably at a higher relative humidity of ~20% (Fig. S10†). Therefore, some modifications such as introducing a hydrophobic diffusion layer could be made aiming to further enhance their practical applications.²⁵

Fig. 3a and b show a good stretchability of the Li-air battery. The discharge voltage plateau can be well maintained after stretching with a strain up to 100% (Fig. 3c), and a red light-emitting diode (LED) powered by the Li-air battery also exhibited stable luminance after stretching (Fig. 3c, inset). The electrochemical performance of the battery was also elucidated using electrochemical impedance spectra. As expected, both ohmic resistance and interfacial charge transfer resistance remained almost unchanged after stretching with increasing strains to 100% (Fig. 3d). The voltage profiles were further traced during a dynamically stretching process with increasing speeds. A stable dynamic performance can be observed from Fig. 3e even at a stretching speed as high as 1.6 cm s⁻¹, and the voltage undulation was recorded to be less than 1%. Fig. 3f and g present that the voltage profiles were also stable under other

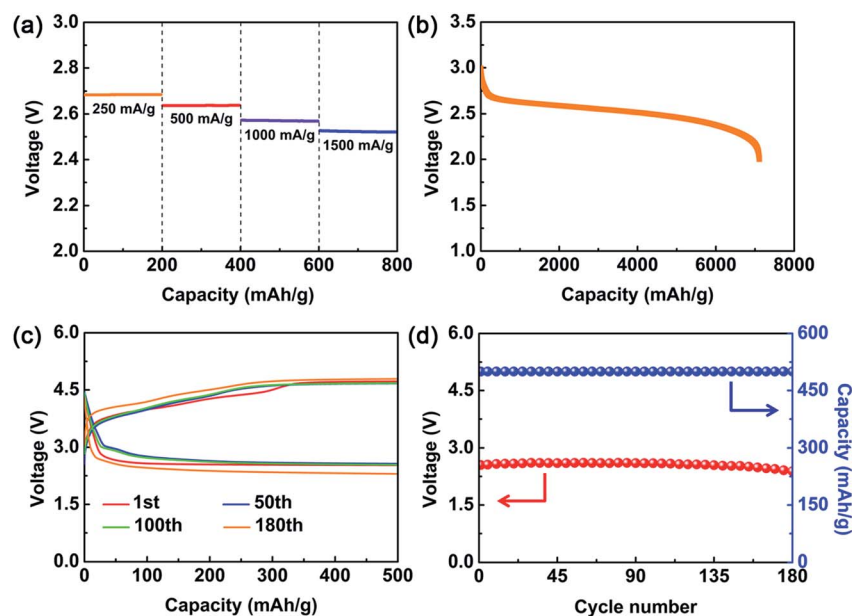


Fig. 2 Electrochemical performances of the stretchable Li-air battery. (a) Rate capability at increasing current densities. (b) Galvanostatic discharge curves at a current density of 500 mA g⁻¹. (c and d) Charge and discharge curves and the corresponding cycling performance at a current density of 1000 mA g⁻¹, respectively. The electrochemical properties were normalized on the weight of CNTs.

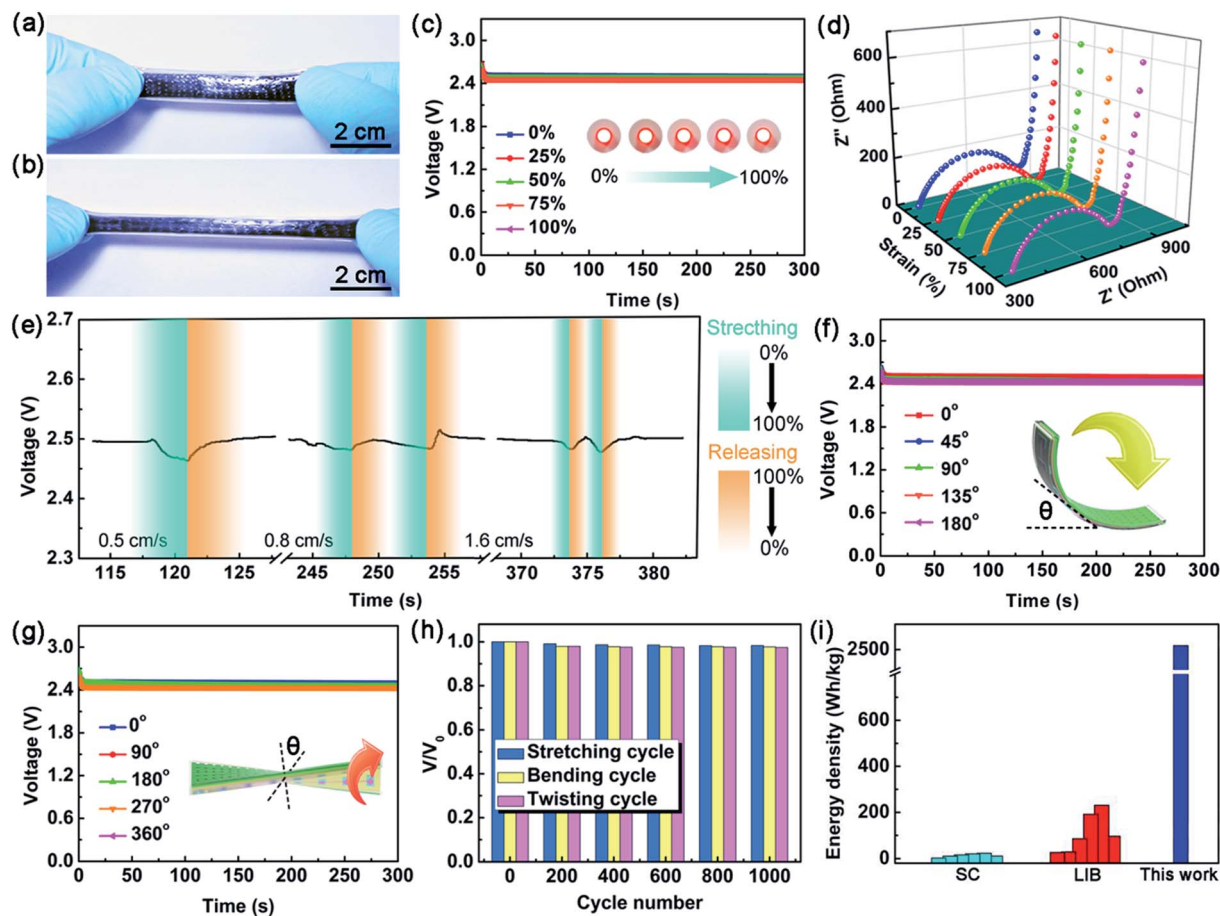


Fig. 3 Flexibility and stretchability of the Li-air battery. (a and b) Photographs of the stretchable Li-air battery before and after stretching, respectively. (c) Discharge curves of the stretchable Li-air battery under increasing strains. The inserted photographs display a red LED lit up by the Li-air battery under increasing strains. (d) Electrochemical impedance spectra of the stretchable Li-air battery under increasing strains. (e) Discharge curve under a dynamic stretching/releasing process at increasing stretching/releasing speeds. (f and g) Discharge curves of the stretchable Li-air battery under bending and twisting with increasing angles, respectively. (h) Dependence of discharge voltage on the stretching cycle at a strain of 75%, bending cycle at a bending angle of 90° and twisting cycle at a twisting angle of 180°, respectively. V_0 and V correspond to the discharge voltage plateau before and after deforming, respectively. (i) energy densities of representative stretchable energy storage devices. SC: supercapacitors; LIB: lithium-ion battery.^{13,26–36} The discharge curves were measured at a current density of 1000 mA g⁻¹.

deformations, *e.g.*, bending and twisting. In addition, the electrochemical performances were all well maintained after stretching, bending and twisting, each for 1000 cycles (Fig. 3h and S11†).

The stretchable Li-air battery exhibited a high specific capacity of 7111 mAh g⁻¹, which is over 61 times that of stretchable lithium-ion battery derived from LiCoO₂ and graphite,¹³ 59 times that of LiFePO₄ and Li₄Ti₅O₁₂,²⁶ and 79 times that of LiMn₂O₄ and Li₄Ti₅O₁₂.²⁷ Furthermore, the energy density based on the total weight of the air electrode and resultant Li₂O₂ reached 2540 Wh kg⁻¹, which is about 22 times higher than that of previous stretchable lithium-ion batteries and 110 times than that of stretchable supercapacitors (Fig. 3i).^{13,26–36} Additionally, the specific capacity and energy density of the stretchable Li-air battery were comparable to the previous rigid and flexible Li-air (oxygen) batteries (Table S1†).

Benefiting from its high capacity and energy density, a stretchable Li-air battery with 0.14 mg of the air electrode

was able to power a blue LED (ignition voltage of ~2.5 V) for more than 12 h (Fig. 4a). The discharge voltage plateau can be further increased to ~5.2 and ~7.8 V when two and three stretchable Li-air batteries were assembled in series, respectively. Due to its high flexibility, the stretchable Li-air battery shows immense potential for wearable applications.^{37–39} For instance, a wearable physiological monitoring system was constructed by integrating two stretchable Li-air batteries with a sensor suite (Fig. 4c and S12†). This device presents a self-adaption size *via* elastic deformation of the “energetic straps” (Fig. 1a), and can therefore be easily worn on the head of people (Fig. 4d) to collect different physiological signals such as eye blinks, jaw clenches and light muscle tension (Fig. 4e). Furthermore, the stretchable Li-air battery was woven into a flexible powering textile, which can effectively and stably power an LED in different deformations (Fig. 4f–h).

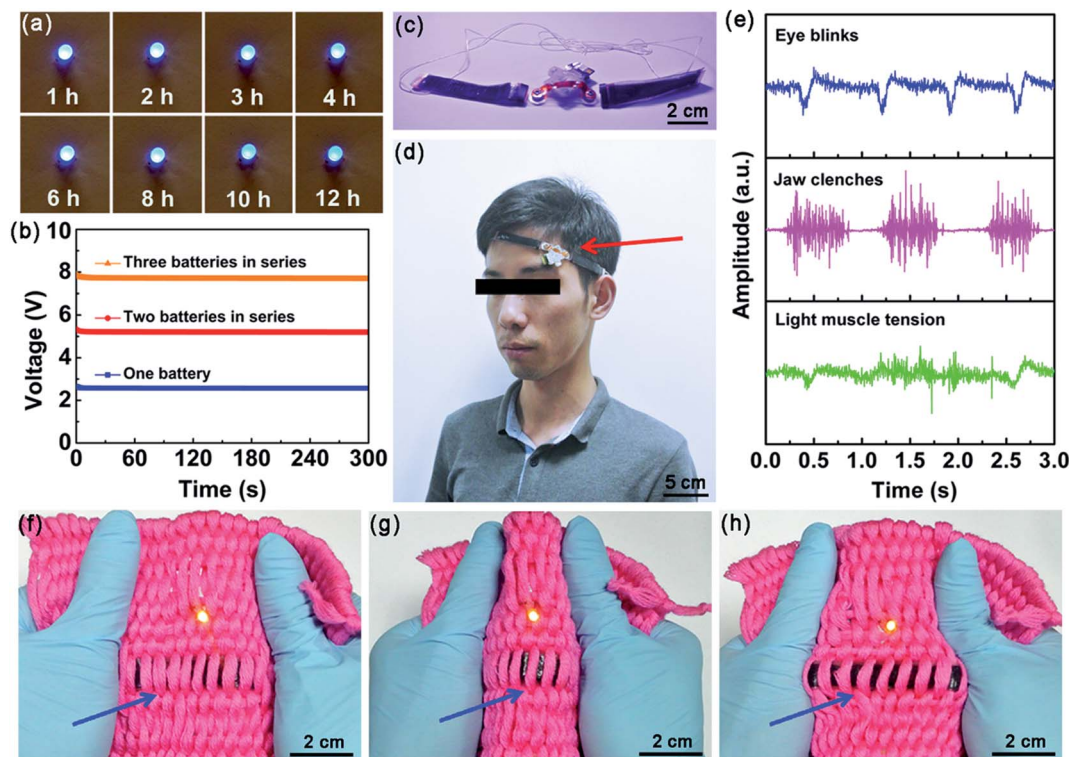


Fig. 4 Wearable applications of the stretchable Li-air battery. (a) A blue LED lit up by a stretchable Li-air battery for 12 h. (b) Discharging curves of stretchable Li-air batteries connected in series. It was measured at a current density of 1000 mA g^{-1} . (c) Photograph of a wearable physiological monitoring system. The corresponding schematic illustration is shown in Fig. 1a (d) photograph of the wearable physiological monitoring system worn on the head of a person to monitor the physiological signals. The red arrow indicates the wearable physiological monitoring system. (e) Different physiological signals collected using the wearable physiological monitoring system. (f–h) Photograph of a stretchable Li-air battery woven into textile to power a yellow LED under deformations. Blue arrows indicate the stretchable Li-air battery.

Conclusion

In conclusion, we have developed a flexible and stretchable Li-air battery that exhibits a high electrochemical performance. The Li-air battery is demonstrated to be promising for a variety of applications, and the use of it for wearable electronic devices has been carefully presented with high efficiency. This work also represents a new and general strategy in the advancement of the next-generation power systems.

Acknowledgements

This work was supported by NSFC (21225417, 51573027, and 51403038), STCSM (15XD1500400, 12nm0503200, and 15JC1490200) and the Program for Outstanding Young Scholars from Organization Department of the CPC Central Committee.

References

- M. Vosgueritchian, J. B.-H. Tok and Z. Bao, *Nat. Photonics*, 2013, 7, 769.
- H. Lee, T. K. Choi, Y. B. Lee, H. R. Cho, R. Ghaffari, L. Wang, H. J. Choi, T. D. Chung, N. Lu, T. Hyeon, S. H. Choi and D. H. Kim, *Nat. Nanotechnol.*, 2016, 11, 566.
- C. Xie, J. Liu, T. M. Fu, X. Dai, W. Zhou and C. M. Lieber, *Nat. Mater.*, 2015, 14, 1286.
- Z. Zhang, K. Guo, Y. Li, X. Li, G. Guan, H. Li, Y. Luo, F. Zhao, Q. Zhang, B. Wei, Q. Pei and H. Peng, *Nat. Photonics*, 2015, 9, 233.
- A. M. Zamarayeva, A. M. Gaikwad, I. Deckman, M. Wang, B. Khau, D. A. Steingart and A. C. Arias, *Adv. Electron. Mater.*, 2016, 2, DOI: 10.1002/aelm.201500296.
- Y. H. Lee, J. S. Kim, J. Noh, I. Lee, H. Kim, S. Choi, J. Seo, S. Jeon, T. S. Kim, J. Y. Lee and J. Choi, *Nano Lett.*, 2013, 13, 5753.
- M. Kaltenbrunner, G. Kettlgruber, C. Siket, R. Schwödauier and S. Bauer, *Adv. Mater.*, 2010, 22, 2065.
- C. Yan, X. Wang, M. Cui, J. Wang, W. Kang, C. Y. Foo and P. S. Lee, *Adv. Energy Mater.*, 2014, 4, DOI: 10.1002/aenm.201301396.
- A. M. Gaikwad, A. M. Zamarayeva, J. Rousseau, H. Chu, I. Derin and D. A. Steingart, *Adv. Mater.*, 2012, 24, 5071.
- T. Chen, R. Hao, H. Peng and L. Dai, *Angew. Chem., Int. Ed.*, 2015, 54, 618.
- Y. Huang, J. Tao, W. Meng, M. Zhu, Y. Huang, Y. Fu, Y. Gao and C. Zhi, *Nano Energy*, 2015, 11, 518.
- Z. Song, X. Wang, C. Lv, Y. An, M. Liang, T. Ma, D. He, Y. J. Zheng, S. Q. Huang, H. Yu and H. Jiang, *Sci. Rep.*, 2015, 5, 10988.

- 13 S. Xu, Y. Zhang, J. Cho, J. Lee, X. Huang, L. Jia, J. A. Fan, Y. Su, J. Su, H. Zhang, H. Cheng, B. Lu, C. Yu, C. Chuang, T. I. Kim, T. Song, K. Shigeta, S. Kang, C. Dagdeviren, I. Petrov, P. V. Braun, Y. Huang, U. Paik and J. A. Rogers, *Nat. Commun.*, 2013, **4**, 1543.
- 14 G. Kettlgruber, M. Kaltenbrunner, C. M. Siket, R. Moser, I. M. Graz, R. Schwödiauer and S. Bauer, *J. Mater. Chem. A*, 2013, **1**, 5505.
- 15 P. G. Bruce, S. A. Freunberger, L. J. Hardwick and J. M. Tarascon, *Nat. Mater.*, 2012, **11**, 19.
- 16 A. C. Luntz and B. D. McCloskey, *Chem. Rev.*, 2014, **114**, 11721.
- 17 T. Liu, M. Leskes, W. Yu, A. J. Moore, L. Zhou, P. M. Bayley, G. Kim and C. P. Grey, *Science*, 2015, **350**, 530.
- 18 Y. Zhang, L. Wang, Z. Guo, Y. Xu, Y. Wang and H. Peng, *Angew. Chem., Int. Ed.*, 2016, **55**, 4487.
- 19 H. D. Lim, B. Lee, Y. Zheng, J. Hong, J. Kim, H. Gwon, Y. Ko, M. Lee, K. Cho and K. Kang, *Nat. Energy*, 2016, **1**, 16066.
- 20 Q. Liu, J. Xu, D. Xu and X. Zhang, *Nat. Commun.*, 2015, **6**, 7892.
- 21 H. D. Lim, H. Song, J. Kim, H. Gwon, Y. Bae, K. Y. Park, J. Hong, H. Kim, T. Kim, Y. H. Kim, X. Lepro, R. Ovalle-Robles, R. H. Baughman and K. Kang, *Angew. Chem., Int. Ed.*, 2014, **53**, 3926.
- 22 T. Zhang and H. Zhou, *Nat. Commun.*, 2013, **4**, 1817.
- 23 J. Yi, X. Liu, S. Guo, K. Zhu, H. Xue and H. Zhou, *ACS Appl. Mater. Interfaces*, 2015, **7**, 23798.
- 24 L. Wang, Q. Wu, Z. Zhang, Y. Zhang, J. Pan, Y. Li, Y. Zhao, L. Zhang, X. Cheng and H. Peng, *J. Mater. Chem. A*, 2016, **4**, 3217.
- 25 T. Zhang and H. Zhou, *Angew. Chem., Int. Ed.*, 2012, **124**, 11224.
- 26 W. Liu, Z. Chen, G. Zhou, Y. Sun, H. R. Lee, C. Liu, H. Yao, Z. Bao and Y. Cui, *Adv. Mater.*, 2016, **28**, 3578.
- 27 W. Weng, Q. Sun, Y. Zhang, S. He, Q. Wu, J. Deng, X. Fang, G. Guan, J. Ren and H. Peng, *Adv. Mater.*, 2015, **27**, 1363.
- 28 Z. Niu, H. Dong, B. Zhu, J. Li, H. H. Hng, W. Zhou, X. Chen and S. Xie, *Adv. Mater.*, 2013, **25**, 1058.
- 29 X. Chen, H. Lin, P. Chen, G. Guan, J. Deng and H. Peng, *Adv. Mater.*, 2014, **26**, 4444.
- 30 J. Yu, W. Lu, S. Pei, K. Gong, L. Wang, L. Meng, Y. Huang, J. P. Smith, K. S. Booksh, Q. Li, J. H. Byun, Y. Oh, Y. Yan and T. W. Chou, *ACS Nano*, 2016, **10**, 5204.
- 31 D. Kim, G. Shin, Y. J. Kang, W. Kim and J. S. Ha, *ACS Nano*, 2013, **7**, 7975.
- 32 Y. Xie, Y. Liu, Y. Zhao, Y. H. Tsang, S. P. Lau, H. Huang and Y. Chai, *J. Mater. Chem. A*, 2014, **2**, 9142.
- 33 M. Yu, Y. Zhang, Y. Zeng, M. S. Balogun, K. Mai, Z. Zhang, X. Lu and Y. Tong, *Adv. Mater.*, 2014, **26**, 4724.
- 34 J. Ren, Y. Zhang, W. Bai, X. Chen, Z. Zhang, X. Fang, W. Weng, Y. Wang and H. Peng, *Angew. Chem., Int. Ed.*, 2014, **53**, 7864.
- 35 Y. Zhang, W. Bai, J. Ren, W. Weng, H. Lin, Z. Zhang and H. Peng, *J. Mater. Chem. A*, 2014, **2**, 11054.
- 36 Y. Zhang, W. Bai, X. Cheng, J. Ren, W. Weng, P. Chen, X. Fang, Z. Zhang and H. Peng, *Angew. Chem., Int. Ed.*, 2014, **53**, 14564.
- 37 W. Zeng, L. Shu, Q. Li, S. Chen, F. Wang and X. M. Tao, *Adv. Mater.*, 2014, **26**, 5310.
- 38 W. Gao, S. Emaminejad, H. Y. Y. Nyein, S. Challa, K. Chen, A. Peck, H. M. Fahad, H. Ota, H. Shiraki, D. Kiriya, D. H. Lien, G. A. Brooks, R. W. Davis and A. Javey, *Nature*, 2016, **529**, 509.
- 39 T. Yokota, P. Zalar, M. Kaltenbrunner, H. Jinno, N. Matsuhisa, H. Kitanosako, Y. Tachibana, W. Yukita, M. Koizumi and T. Someya, *Sci. Adv.*, 2016, **2**, e1501856.